Research Article

Modeling of Moisture Content of Subgrade Materials in High-Speed Railway Using a Deep Learning Method

LiLei Chen,[1] Jing Chen [ID],[1] Chao Wang,[1] Yanhua Dai,[1,2] Rongyan Guo,[1] and Qian Huang[1,2]

[1]*College of Civil Engineering, Shaoxing University, Shaoxing 312000, China*
[2]*Key Laboratory of Rock Mechanics and Geohazards of Zhejiang Province, Shaoxing 312000, China*

Correspondence should be addressed to Jing Chen; jingchen.sxu@gmail.com

Moisture content of subgrade materials is an essential factor affecting frost heave deformation of high-speed railway subgrade in a seasonally frozen region. Modeling and predicting moisture transport play an important role in analyzing the subgrade thermal and hydraulic conditions in cold regions. In this study, a long short-term memory (LSTM) model was proposed based on subgrade material moisture in two sections during one winter and spring cycle from 2015 to 2016. The reliability of the model was verified by comparing the monitoring data with the model results. The results demonstrate that the LSTM model can be effectively used to forecast the dynamic characteristics of the moisture of subgrade materials. The data of simulated moisture content of subgrade materials have a root mean square error ranging from 0.17 to 0.47 in the training phase and from 0.20 to 10.5 in the testing phase. The proposed model provides a novel method for long-term moisture prediction in subgrade materials of high-speed railways in cold regions.

1. Introduction

Seasonally frozen ground is mainly distributed in high-latitude areas such as northeast China, north China, and northwest China, accounting for 53.5% of China's total land area [1, 2]. Subgrade materials in cold regions undergo several freeze-thaw cycles every year, leading to subgrade degradation [3–5]. The frost heave problem of high-speed railway foundations in seasonally frozen regions has garnered significant attention and research interest from experts and scholars. Through field monitoring and laboratory tests, it was found that soil properties, temperature, and moisture content were the main factors affecting the frost heave of the subgrade [6–13]. Zhang et al. [14] performed indoor frost heaving tests under different moisture contents for five types of coarse-grained soils and 13 types of fine-grained soils. The results demonstrated that moisture content was the most important factor causing frost heaving [15].

The variation in the moisture content of subgrade materials is affected by climate, thermal properties of soil particles, loading conditions, and soil texture [16–19]. Several experiments and numerical models have focused on one or two controlling factors that may affect moisture transport. However, they are time-consuming and sometimes cannot predict the long-term dynamics of moisture content, for instance, Khoury et al. [20] found that a change in the subgrade moisture content affected the performance of pavement materials. Naji et al. [21] used a mathematical model to predict the relationship between soil elastic modulus and moisture content. They used the model to predict the change in pavement bearing capacity caused by seasonal changes in moisture content. Through on-site monitoring, Lin et al. [22] found that moisture content change was related to the nature of subgrade filling. However, few studies have simulated and predicted the moisture variation in high-speed railway subgrades in cold regions.

Deep learning methods based on artificial neural networks can quickly extract effective data features from massive monitoring data and analyze the nonlinear change relationship of monitoring data, which can thereafter be used to effectively predict the change in subgrade moisture

content; therefore, artificial neural network has been widely used in the overall evaluation of subgrade engineering [23]. The long and short-term network is a special recursive neural network that can solve complex problems and learn fast [24]. For instance, Chen et al. [25] used this model to predict the dynamic swelling deformation of a high-speed railway subgrade.

The embankment of the Lanzhou–Xinjiang high-speed railway, located in northwest China, has been operating since December 2014. The mean annual air temperature is approximately 4.8°C at the Minle weather station near the monitoring site. The highest and lowest temperatures were 35.0 and −31.5°C, respectively. The annual mean rainfall was recorded as 381.2 mm, whereas the annual mean evaporation was 1623.0 mm in 2015. The start and end dates of snowfall were September 30, 2015, and May 19, 2016, respectively. The recorded maximum natural snow depth was 220 mm, whereas the recorded maximum natural frozen depth was 184 cm from 2015 to 2016 [22].

In this study, the long short-term memory (LSTM) model was established to simulate long-term moisture changes in subgrade materials. We examined the applicability of the LSTM model to the prediction of time-series data of the moisture of subgrade materials in high-speed railways and compared field monitoring data and model outputs.

2. Methods

The subgrade of the Lanzhou–Xinjiang high-speed railway consists of four main layers: a 0.4 m height concrete layer, 0.5 m height nonfrost susceptible crushed rock layer, 1.8 m height low-frost susceptible crushed rock layer, and an underlying soil layer. In this study, two monitoring sections of subgrade, K2020 + 024 and K2028 + 746, were selected, and their moisture contents were measured using a gravimetric method with six soil moisture sensors [22] (Figure 1). The data were recorded at 4 h intervals from August 2015 to April 2016. The measuring method and working principle of the soil moisture sensors were the same as those of Mittelbach et al. [26]. The moisture sensor was a QSY8909A moisture sensor produced by Sichuan Qishiyuan Science and Technology Co., Ltd. Its measuring range was 0–100%, length was 6 cm, diameter was 3 mm, probe material was stainless steel, and temperature range was −25–80°C [27].

In the K 2020 + 024 and K 2028 + 746 sections in the concrete layer, the moisture content of 0.2 m soil started to fluctuate slightly. Subsequently, it began to decline rapidly and tended to be constant in December 2015. It began to fluctuate again in late March 2016. The moisture content of 0.5 m soil began to fluctuate and rise, reached a peak in February 2016, and thereafter began to fluctuate and descend. In nonfrost susceptible A/B fillings, and the variation trend of moisture content at 1.0 m was approximately the same as that at 0.5 m.

As shown in Figure 2, the soil moisture content is affected by temperature, rainfall, and other factors. Its monitoring data have some noise and exhibit prominent

nonlinear characteristics; therefore, it is difficult to predict them.

In this study, there are missing values in the data due to the communication failure of detection equipment and other factors. For missing data, detection data between adjacent time points were used for interpolation processing. To accelerate the convergence rate of the model, the data were normalized according to the characteristics of the test data and requirements of the LSTM model. The normalization calculation formula is as follows:

$$x_i = \frac{x_i - \min x_i}{\max x_i - \min x_i}, \tag{1}$$

where x_i denotes the moisture content monitoring data, whereas $\min x_i$ and $\max x_i$ represent the minimum and maximum values of x_i, respectively [23].

The LSTM model [23] is a neural network model proposed by Hochreiter in the 1990s; its model structure is as shown in Figure 3. It contains a particular unit, namely, the memory block in the recursive hidden layer. The memory block includes a cell state and three gated mechanisms (input, forget, and output gates) for controlling the flow of information. The sigmoid function implements a gating mechanism. After the data flows in, they first enter the forget gate. After part of the redundant information is discarded to obtain the critical feature data, the data enter the input gate to control the data update. Finally, they pass through the output gate as output. The mathematical expression for this process is as follows.

First, the forget gate f_t calculates the cell state that needs to be retained at the previous moment through the activation function as follows [23]:

$$i_f = \sigma\left(W_f \cdot [h_{t-1}, x_t] + b_f\right), \tag{2}$$

where W_f and b_f denote the weight matrix and bias of the forget gate, respectively, σ denotes the sigmoid function, and h_{t-1} represents the output at moment $t - 1$ [23].

Second, the input gate i_t retains information regarding the current input x_t to be updated to the current cell state C_t as follows [23]:

$$i_t = \sigma\left(W_i \cdot [h_{t-1}, x_t] + b_i\right). \tag{3}$$

Thereafter, the output gate o_t controls the information that comes out as follows [23]:

$$o_t = \sigma\left(W_o \cdot [h_{t-1}, x_t] + b_o\right). \tag{4}$$

Based on the previous input and output information, the following formula can be used to calculate the nonlinear output [23]:

$$\widetilde{C}_t = \tanh\left(W_c \cdot [h_{t-1}, x_t] + b_c\right). \tag{5}$$

Finally, the new cell state can be expressed as follows [23]:

$$\begin{aligned} C_t &= f_t * C_{t-1} + i_t * \widetilde{C}_t, \\ h_t &= o_t * \tanh(C_t). \end{aligned} \tag{6}$$

FIGURE 1: Fieldwork of the automatic monitoring system of moisture content of subgrade materials of high-speed railway in cold regions.

By controlling the input gate, the influence of redundant information can be avoided, and information of the previous time is retained in the network owing to the forgetting gate. This model addresses long-term dependence and gradient disappearance problems encountered by traditional recurrent neural networks in prediction tasks, and it is now widely used in time-series forecasting [25, 28, 29].

In this study, root mean square error (RMSE) and R-score (R^2) were used to evaluate the performance of the model. The smaller the RMSE value calculated, the closer the R^2 value is to 1 and the higher the accuracy and reliability of the model prediction. The specific formula is as follows:

$$\text{RMSE} = \sqrt{\frac{1}{n} \sum_{i=1}^{n} (y_i - \hat{y}_i)^2},$$

$$R^2 = 1 - \frac{\sum_{i=1}^{n} (y_i - \hat{y}_i)^2}{\sum_{i=1}^{n} (y_i - \overline{y}_i)^2}, \quad (7)$$

where n denotes the number of predicted samples, whereas y_i, $\overline{y}_i$, and $\hat{y}_i$ denote the measured values, mean of the measured values, and predicted value, respectively.

3. Results and Discussion

The training of the LSTM model requires the monitoring data to be preprocessed. In this study, according to the commonly used split ratio, the holdout method was used to split the dataset, with the training set accounting for 80% and validation set accounting for 20%. The monitoring data of August 1, 2015, solstice on February 11, 2016, were used as the training set, whereas the detection data of February 12, 2016, solstice on March 31, 2016, were used as the validation set. The training set was used to train the weight of the model, whereas the validation set was used to evaluate the model performance. Because the selection of hyperparameters has a significant impact on the performance of the model [30], it is necessary to set the hyperparameters of the model before the training begins. In this study, the number of cells in the LSTM model was considered as the critical hyperparameter, and the candidate operations of the hyperparameter was [5, 10, 20, 30, 40, 50]. To accurately evaluate the performance of the model on the specified

parameter performance and avoid the instability of the performance of a single training session, the average error of five repeated training sessions was used as the evaluation indicator. The error statistics of the hyperparameter search training are as shown in Figure 4. It is observed from the figure that when the number of units is 10, the model has a minor error and higher computational efficiency. After several experiments, the number of units in the model was determined to be 10, the epoch was set to 200, and learning rate was 0.001. The model was implemented using TensorFlow framework. In this study, the gradient descent algorithm was applied to update the weight of the model. The adaptive moment (Adam) estimation was selected as the optimization algorithm for the training process of the model. In comparison with other optimization algorithms, the Adam algorithm is more efficient in terms of calculation and it has a better effect in practical applications [31].

The calculated results of R^2 and RMSE indices on the training and validation sets of the trained model are summarized in Table 1. From the table, the prediction effect of the LSTM model is the best when the depth of the LSTM model in R^2 of section K2028 reaches 0.94. In the training set of moisture content at all depths, R^2 was greater than 0.95, indicating that the model fitted the training data well. However, there was a gap between R^2 in the test and training sets, indicating that the model had an overfitting phenomenon. The RMSE error of the model is small for each moisture content dataset, thereby proving that the LSTM model is suitable for the prediction of soil moisture content and it has a specific application potential.

To more intuitively compare the prediction effect of the model on different moisture contents, a comparison between the predicted value of the model and the measured value on the two sections, K2020 + 024 and K2028 + 746, is as shown in Figures 5 and 6. It is observed from Figure 4 and Table 1 that the prediction accuracy of the model decreases with an increase in depth possibly because the change in soil moisture content is a gradual accumulation process, and the change in the soil moisture content in a period of shallow depth is easier to learn from the historical trend. With the increase in the predicted time steps, the deviation of soil moisture content at a depth of 1.0 m in the two sections increases, and the model's prediction ability is weak.
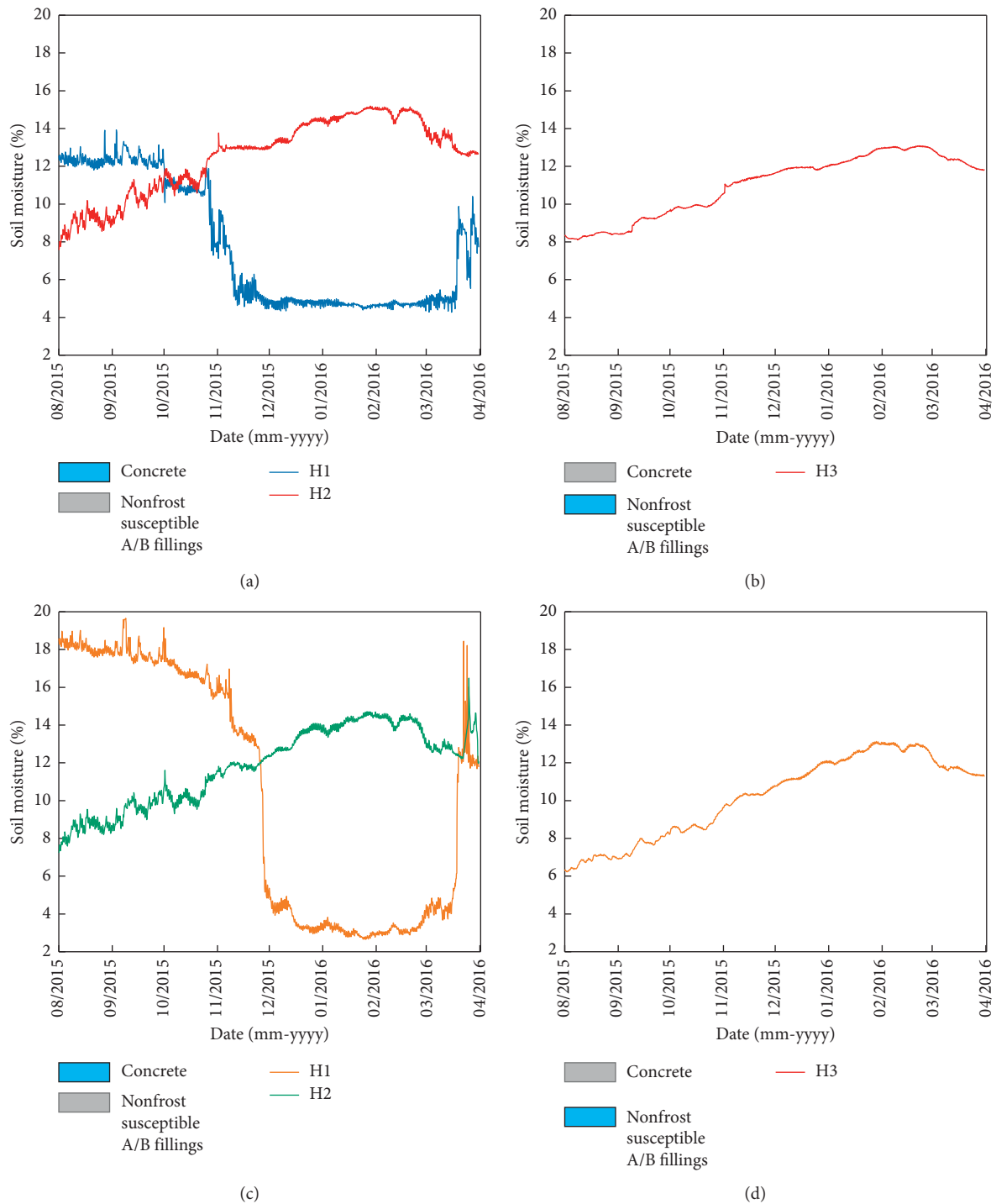
(a)

(b)

(c)

(d)

Figure 2: Variations in moisture content were measured at three depths in two sections from August 2015 to March 2016. *Note.* H1 to H3 represents depth of 0.2, 0.5, and 1.0 m, respectively. (a-b) K 2020 + 024 section. (c-d) K 2028 + 746 section.

In this study, we use an LSTM model to predict the moisture content of subgrade materials in high-speed railways based on one-year field monitoring data. The model achieved great performance for predicting moisture content of subgrade materials above 0.5 m in the two sections. However, we found that the prediction accuracy of the moisture content of subgrade materials below 0.5 m was slightly lower than those of others. This phenomenon may be attributed to the sample size and model parameters [32]. In addition, our model does not consider the detailed influential factors of soil moisture and soil particle structure, which may affect the model outputs.
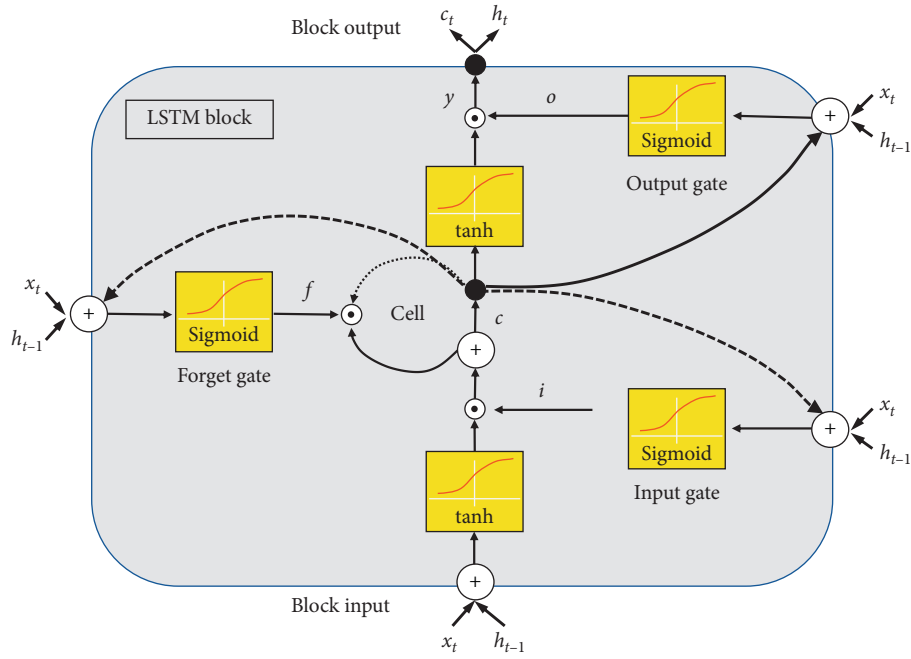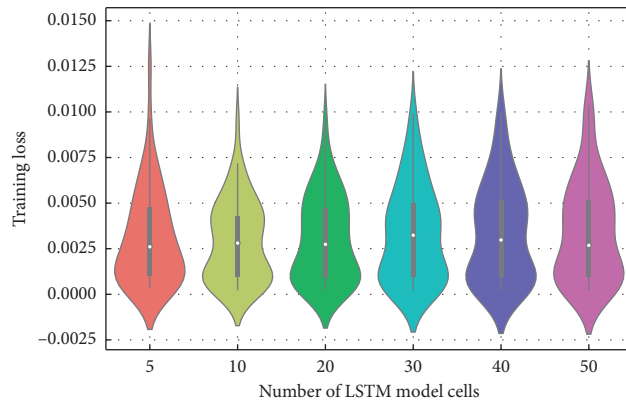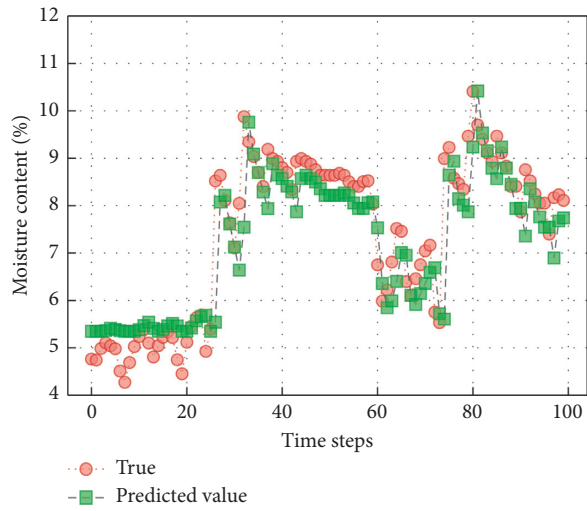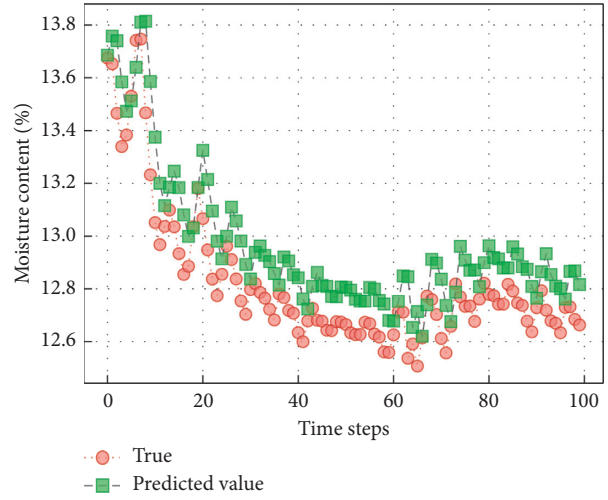
Figure 3: LSTM model structure.

Figure 4: Training loss LSTM model with different number of units.

Table 1: Performance evaluation index of the model.

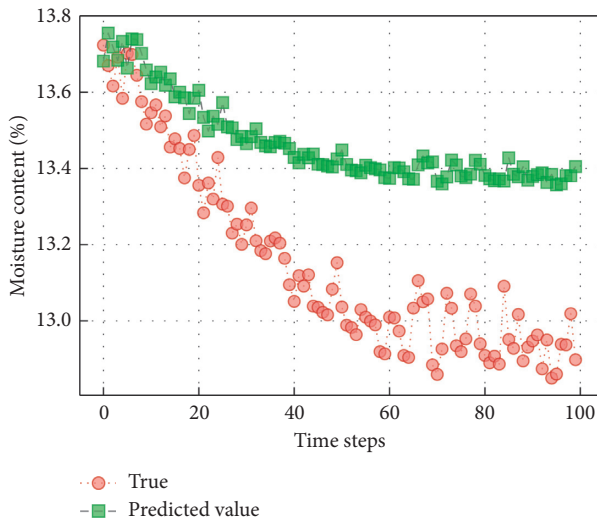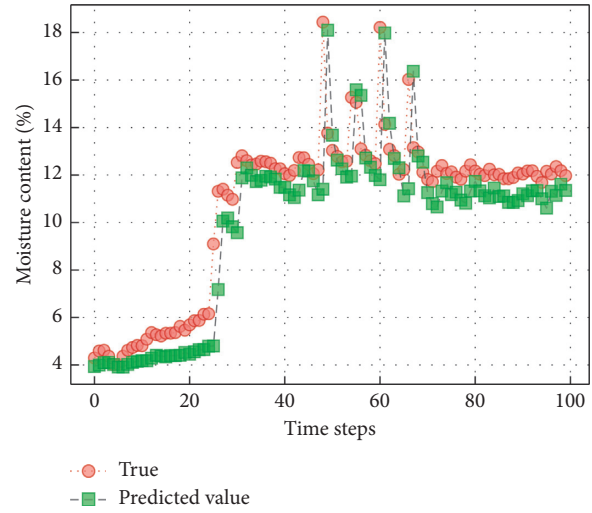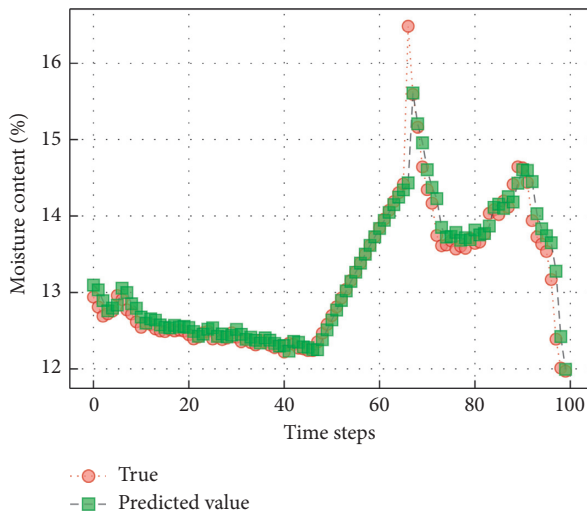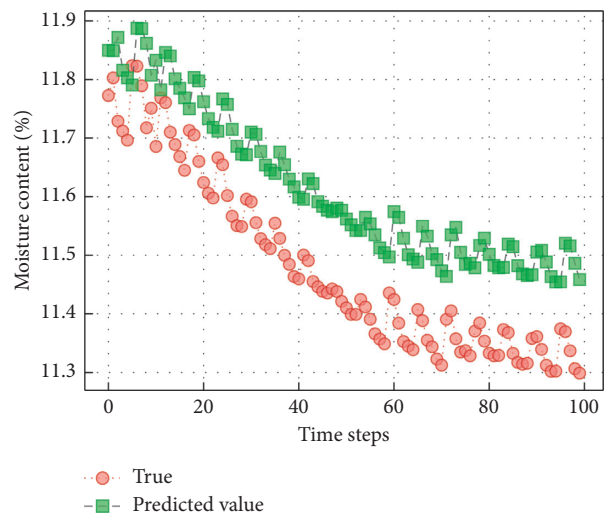| Section	R^2		RMSE	
	Train set	Test set	Train set	Test set
K2020 + 024 H1	0.99	0.90	0.36	0.51
K2020 + 024 H2	0.98	0.92	0.31	0.24
K2020 + 024 H3	0.95	0.87	0.17	0.21
K2028 + 746 H1	0.99	0.93	0.47	1.05
K2028 + 746 H2	0.99	0.94	0.23	0.20
K2028 + 746 H3	0.98	0.89	0.28	0.20

Figure 5: Predicting results of two subgrade sections in the three depths. (a–c) K 2020 + 024 section. (d–f) K 2028 + 746 section.
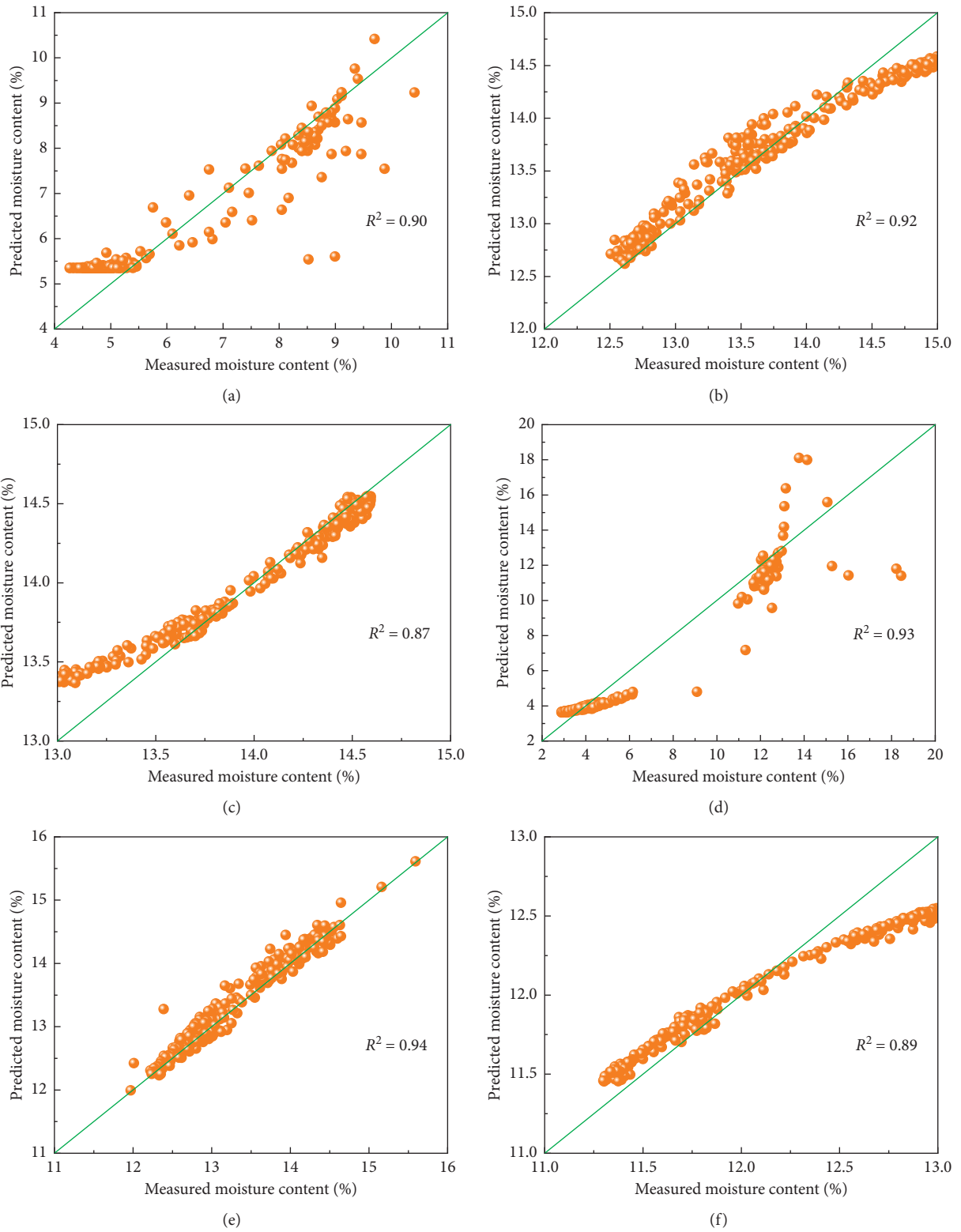
FIGURE 6: Comparison of the predicted values of the soil moisture with measured values (a–c) K 2020 + 024 section. (d–f) K 2028 + 746 section.

4. Conclusions

Based on soil moisture measurement data at different depths of two sections of the Lan–Xin high-speed railway and combined with the LSTM deep neural network model, this study explored the application of this model in the short-term prediction of temporal series changes in soil moisture content. The specific conclusions are as follows:

(1) Aiming at obtaining a nonlinear law for soil moisture monitoring data, the number of model units was determined using the hyperparameter search method

(2) The LSTM neural network model has a strong generalization ability in the short-term prediction of soil moisture content, and it can be used for soil moisture content prediction tasks

(3) For a significant number of soil moisture prediction tasks at different depths, the LSTM model has higher prediction accuracy in the shallower depth; it has the best prediction effect for the depth of 0.5 m in a specific time period

In conclusion, the strategy discussed in this study, based on field monitoring data and a deep neural network model, can effectively extract the dynamic characteristics of soil moisture content monitoring. It can effectively predict the soil moisture content in a specific period of time, thereby providing a practical reference for the safety of train operation.

Data Availability

The figures and tables data used to support the findings of this study are included within the article.

Conflicts of Interest

The authors declare that they have no conflicts of interest.

Acknowledgments

References

[1] X. Xu, J. Wang, and L. Zhang, *Physics of Frozen Soil*, Science Press, Beijing, China, 2nd edition, 2010.

[2] T. Zhang, R. G. Barry, K. Knowles, J. A. Heginbottom, and J. Brown, "Statistics and characteristics of permafrost and ground-ice distribution in the northern hemisphere1," *Polar Geography*, vol. 23, no. 2, pp. 132–154, 1999.

[3] B. Tai, Z. Yue, T. Sun, S. Qi, L. Li, and Z. Yang, "Novel anti-frost subgrade bed structures a high speed railways in deep seasonally frozen ground regions: experimental and numerical studies," *Construction and Building Materials*, vol. 269, Article ID 121266, 2021.

[4] Y. Yu and A. Deng, "Mechanism and prevention of highway distress in seasonal frost area," in *Geotechnical Engineering for Disaster Mitigation and Rehabilitation,* Springer, Berlin, Germany, 2008.

[5] S. Zhang, D. Sheng, G. Zhao, F. Niu, and Z. He, "Analysis of frost heave mechanisms in a high-speed railway embankment," *Canadian Geotechnical Journal*, vol. 53, no. 3, pp. 520–529, 2016.

[6] L. Z. Wu, Q. Xu, and R. Q. Huang, "Analysis of freezing-thawing test process of unsaturated clay," *Rock and Soil Mechanics*, vol. 32, no. 4, pp. 1025–1028, 2011.

[7] S. Li, D. Nie, and J. Wu, "Experimental study on the frost heave and water change of a certain kind of silty clay," *Resource environment and engineering*, vol. 24, no. 5, pp. 615–618, 2010.

[8] P. Li, X. Xu, and F. Chen, "Research status and progress of frozen margin and frost heave model," *Journal of Glaciology and Geocryology*, vol. 22, no. 1, pp. 90–95, 2000.

[9] F. Padilla, J.-P. Villeneuve, and J. Stein, "Simulation and analysis of frost heaving in subsoils and granular fills of roads," *Cold Regions Science and Technology*, vol. 25, no. 2, pp. 89–99, 1997.

[10] T. S. Vinson, F. Ahmad, and R. Rieke, "Factors important to the development of frost heave susceptibility criteria for coarse-grained soils," Transportation Research Board, Washington, DC, USA, 1986, pp. 124–131, Transportation Research Board N1089.

[11] D. Sheng, S. Zhang, and H. E. Zuoyue, "Assessing frost susceptibility of soils," *Chinese Journal of Rock Mechanics and Engineering*, vol. 33, no. 2, pp. 594–605, 2014.

[12] Z. Huixin, W. Zhiqin, and L. Zhaoyu, "Experimental study on frost heave of silty clay in seasonally frost soil regions," *Procedia Engineering*, vol. 28, pp. 282–286, 2012.

[13] H. Liu, F. Niu, Y. Niu, Z. Lin, J. Lu, and J. Luo, "Experimental and numerical investigation on temperature characteristics of high-speed railway's embankment in seasonal frozen regions," *Cold Regions Science and Technology*, vol. 81, pp. 55–64, 2012.

[14] Y. C. Zhang, X. Li, X. F. Zhang, and D. Q. Zhang, "Research on frost heave susceptibility and classification of coarse grained soil of highway subgrade in seasonally frozen ground region," *Yan Tu Gong Cheng Xue Bao*, vol. 29, no. 10, pp. 1522–1526, 2007.

[15] Q. Wang, J. Liu, X. Zhu, J. Liu, and Z. Liu, "The experiment study of frost heave characteristics and gray correlation analysis of graded crushed rock," *Cold Regions Science and Technology*, vol. 126, pp. 44–50, 2016.

[16] N. N. Khoury and M. M. Zaman, "Correlation between resilient modulus, moisture variation, and soil suction for subgrade soils," *Transportation Research Record: Journal of the Transportation Research Board*, vol. 1874, no. 1, pp. 99–107, 2004.

[17] M. Chikira, "Eastward-propagating intraseasonal oscillation represented by chikira-sugiyama cumulus parameterization. part II: understanding moisture variation under weak temperature gradient balance," *Journal of the Atmospheric Sciences*, vol. 71, no. 2, pp. 615–639, 2014.

[18] B. B. Teltayev and E. A. Suppes, "Temperature in pavement and subgrade and its effect on moisture," *Case studies in thermal engineering*, vol. 13, Article ID 100363, 2019.

[19] R. A. Tarefder and M. Ahmad, "Evaluation of pore structure and its influence on permeability and moisture damage in

asphalt concrete," *International Journal of Pavement Engineering*, vol. 18, no. 3, pp. 274–283, 2017.

[20] N. Khoury, R. Brooks, M. M. Zaman, and C. N. Khoury, "Variations of resilient modulus of subgrade soils with postcompaction moisture contents," *Transportation Research Record: Journal of the Transportation Research Board*, vol. 2101, no. 1, pp. 72–81, 2009.

[21] K. Naji, "Resilient modulus-moisture content relationships for pavement engineering applications," *International Journal of Pavement Engineering*, vol. 19, no. 7, pp. 651–660, 2018.

[22] Z. Lin, F. Niu, X. Li et al., "Characteristics and controlling factors of frost heave in high-speed railway subgrade, northwest China," *Cold Regions Science and Technology*, vol. 153, pp. 33–44, 2018.

[23] S. Hochreiter and J. Schmidhuber, "Long short-term memory," *Neural Computation*, vol. 9, no. 8, pp. 1735–1780, 1997.

[24] A. Sagheer and M. Kotb, "Time series forecasting of petroleum production using deep LSTM recurrent networks," *Neurocomputing*, vol. 323, pp. 203–213, 2019.

[25] J. Chen, A. Li, C. Bao et al., "A deep learning forecasting method for frost heave deformation of high-speed railway subgrade," *Cold Regions Science and Technology*, vol. 185, Article ID 103265, 2021.

[26] H. Mittelbach, I. Lehner, and S. I. Seneviratne, "Comparison of four soil moisture sensor types under field conditions in Switzerland," *Journal of Hydrology*, vol. 430-431, pp. 39–49, 2012.

[27] J. Guo, J. Chen, and Y. Hu, "Time series prediction for deformation of the metro foundation pit based on wavelet intelligence model," *Chinese Rock and Soil Mechanics*, vol. 41, no. 1, pp. 299–304, 2020.

[28] Y. Tian and L. Pan, "Predicting short-term traffic flow by long short-term memory recurrent neural network," in *Proceedings of the 2015 IEEE International Conference on Smart city/SocialCom/SustainCom (SmartCity)*, pp. 153–158, IEEE, Chengdu, China, December 2015.

[29] D. M. Nelson, A. C. Pereira, and R. A. De Oliveira, "Stock market's price movement prediction with LSTM neural networks," in *Proceedings of the 2017 International Joint Conference on Neural Networks (IJCNN)*, pp. 1419–1426, IEEE, Anchorage, AK, USA, May 2017.

[30] W. Tian, Z. Liao, and J. Zhang, "An optimization of artificial neural network model for predicting chlorophyll dynamics," *Ecological Modelling*, vol. 364, pp. 42–52, 2017.

[31] D. P. Kingma and J. Ba, "Adam: a method for stochastic optimization," 2014, https://arxiv.org/abs/1412.6980.

[32] F. Zhang, S. Wu, J. Liu et al., "Predicting soil moisture content over partially vegetation covered surfaces from hyperspectral data with deep learning," *Soil Science Society of America Journal*, 2020.